Supporting Information for

Cu(I) complex bearing a PNP-pincer-type phosphaalkene ligand with a bulky fused-ring Eind group: Properties and applications to FLP-type bond activation and catalytic CO_2 reduction

Katsuhiko Takeuchi,*[a] Yuto Tanaka,[b] Ippei Tanigawa,[b] Fumiyuki Ozawa,[b] and Jun-Chul Choi*[a]

[a] National Institute of Advanced Industrial Science and Technology (AIST), Tsukuba, Ibaraki 305-8565, Japan.

[b] International Research Center for Elements Science (IRCELS), Institute for Chemical Research & IRCCS, Kyoto University, Uji, Kyoto 611-0011, Japan.

E-mail: takeuchi-k@asit.go.jp; junchul.choi@aist.go.jp

Contents

Table S1. Crystal Data and Details of the Crystal Structure Determination for **2**, **3**·OEt_2, **5**, and **6**.
Table S2. Cartesian coordinates of the optimized structure of model complex **A**.
Table S3. Cartesian coordinates of the optimized structure of model complex **B**.
Fig. S1. ^{1}H NMR spectrum of **2**.
Fig. S2. ^{13}C NMR spectrum of **2**.
Fig. S3. ^{19}F NMR spectrum of **2**.
Fig. S4. ^{31}P NMR spectrum of **2**.
Fig. S5. ^{1}H NMR spectrum of **3**·OEt_2.
Fig. S6. ^{13}C NMR spectrum of **3**·OEt_2.
Fig. S7. ^{19}F NMR spectrum of **3**·OEt_2.
Fig. S8. ^{31}P NMR spectrum of **3**·OEt_2.
Fig. S9. ^{1}H NMR spectrum of **5**.
Fig. S10. ^{13}C NMR spectrum of **5**.
Fig. S11. ^{19}F NMR spectrum of **5**.
Fig. S12. ^{31}P NMR spectrum of **5**.
Fig. S13. ^{1}H NMR spectrum of **6**.
Fig. S14. ^{13}C NMR spectrum of **6**.
Fig. S15. ^{19}F NMR spectrum of **6**.
Fig. S16. ^{31}P NMR spectrum of **6**.

Table S1. Crystal Data and Details of the Crystal Structure Determination for **2**, **3**·OEt_2, **5**, and **6**

Complex	**2**	**3**·OEt_2	**5**	**6**
Empirical formula	$C_{70}H_{103}CuF_6NP_3$	$C_{47}H_{73}CuF_6NOP_3 \cdot CH_2Cl_2$	$C_{63}H_{97}CuF_6NP_3 \cdot C_6H_{14}$	$C_{71}H_{101}CuF_6NP_3 \cdot 1.5(C_4H_{10}O)$
Formula weight	1228.98	1023.44	1225.04	1350.16
T (K)	103(2)	103(2)	103(2)	103(2)
Crystal system	Triclinic	Triclinic	Triclinic	Monoclinic
Space group	P-1	P-1	P-1	$P2_1/c$
a (Å)	11.873(3)	13.726(2)	10.4742(2)	20.6335(4)
b (Å)	17.868(5)	14.204(2)	17.0519(3)	18.0324(4)
c (Å)	18.028(5)	14.966(3)	19.2242(4)	40.1676(7)
α (°)	113.263(3)	88.769(7)	87.4499(15)	90.00
β (°)	97.23	77.711(6)	85.4988(16)	100.0298(18)
γ (°)	105.296(3)	64.632(5)	76.9395(17)	90.00
V (Å^3)	3273.2(15)	2567.9(7)	3333.14(11)	14716.8(5)
Z	2	2	2	8
d_{calc} (g/cm^3)	1.247	1.324	1.221	1.219
μ(Mo Kα) (mm^{-1})	0.465	0.680	0.456	0.421
F(000)	1316	1080	1320	5800
Crystal size	0.11 x 0.05 x 0.04	0.46 x 0.16 x 0.11	0.12 x 0.08 x 0.03	0.11 x 0.08 x 0.02
θ range (°)	2.1899 to 30.6566	1.9315 to 31.2717	2.1510 to 31.4890	2.2690 to 31.3040
Reflections collected	27772	21536	44549	186189
Independent reflections (R_{int})	11498 (0.0384)	9022 (0.0277)	11676 (0.0334)	24422 (0.1264)
Absorption correction	Multi-scan	Multi-scan	Multi-scan	Multi-scan
Max. and min. transmission	1.0000 and 0.8087	0.9290 and 0.7451	0.9864 and 0.9473	1.00000 and 0.87508
Data / restraints / parameters	11498 / 0 / 771	9022 / 0 / 579	11676 / 10 / 698	24422 / 288 / 1725
GOF on F^2	1.102	1.067	1.047	1.028
$R1$, $wR2$ [$I > 2\sigma(I)$]	0.0531, 0.1221	0.0471, 0.1334	0.0681, 0.1845	0.0655, 0.1499
$R1$, $wR2$ (all data)	0.0688, 0.1398	0.0544, 0.1397	0.0838, 0.2037	0.1164, 0.1796
Largest peak and hole (e Å^3)	0.487 and -0.469	0.750 and -0.675	1.288 and -0.654	1.308 and -0.613

Table S2. Cartesian coordinates of the optimized structure of model complex **A** (dihedral angle of Ph vs P=C = 90°).

38

SCF energy (in vacuo): -1658.76634226 hartree

Cu	0.00005658	-0.48561607	0.00519248
P	2.30821726	-0.24399200	0.00453302
P	-2.30810542	-0.24420162	0.00431025
N	-0.00003374	1.59745416	-0.00455266
C	2.40405692	1.43458531	-0.00612689
H	3.35283900	1.96380796	-0.01091295
C	-2.40411083	1.43436760	-0.00591405
H	-3.35294350	1.96350114	-0.01054340
C	1.18472990	2.25648668	-0.00985756
C	1.20923273	3.65966659	-0.01996127
H	2.15572207	4.18356776	-0.02408816
C	-0.00015941	4.35735349	-0.02479249
H	-0.00020926	5.44012670	-0.03262697
C	-1.20948953	3.65955603	-0.01987001
H	-2.15602609	4.18337203	-0.02397184
C	-1.18485915	2.25638111	-0.00965833
C	3.99074474	-0.90579327	0.00514211
C	4.61971343	-1.22895063	-1.20997553
C	4.65175659	-1.15497375	1.22065099
C	5.90393764	-1.77274546	-1.20531932
H	4.11230246	-1.05464674	-2.15227476
C	5.93558403	-1.69991636	1.21509867
H	4.16919641	-0.92322929	2.16356787
C	6.56167755	-2.00743947	0.00468825
H	6.38794919	-2.01417168	-2.14375305
H	6.44387270	-1.88534726	2.15344177
H	7.55745065	-2.43365194	0.00449792
C	-3.99058300	-0.90614559	0.00522416
C	-4.64988733	-1.15872497	1.22095047
C	-4.62143170	-1.22548339	-1.20993098
C	-5.93383732	-1.70338209	1.21567224
H	-4.16592087	-0.92983527	2.16384716
C	-5.90572711	-1.76910858	-1.20499283
H	-4.11538420	-1.04842465	-2.15244645
C	-6.56174264	-2.00724852	0.00527840
H	-6.44081426	-1.89141961	2.15420554
H	-6.39115394	-2.00769252	-2.14342302
H	-7.55759580	-2.43327384	0.00528186

Table S3. Cartesian coordinates of the optimized structure of model complex **B** (dihedral angle of Ph vs P=C = 0°).

38

SCF energy (in vacuo): -1658.77778389 hartree

Cu	-0.00000158	-0.36208651	0.00005268
P	-2.29907665	-0.11881505	0.00004158
P	2.29907467	-0.11881902	0.00010895
N	-0.00000061	1.71312364	-0.00007954
C	-2.40715487	1.55825785	-0.00002661
H	-3.34495796	2.10401322	-0.00004900
C	2.40715376	1.55825372	0.00000213
H	3.34495708	2.10400876	-0.00002833
C	-1.18713818	2.37165322	-0.00002149
C	-1.20984019	3.77589038	0.00002153
H	-2.15532772	4.30133937	0.00003941
C	0.00000171	4.47169621	0.00001109
H	0.00000255	5.55458811	0.00006004
C	1.20984266	3.77588836	0.00004030
H	2.15533090	4.30133621	0.00008251
C	1.18713839	2.37165140	-0.00001891
C	-3.90186351	-0.90744920	-0.00001045
C	-5.13301390	-0.22149872	-0.00009099
C	-3.90114661	-2.31836767	0.00004236
C	-6.32794086	-0.93202158	-0.00011371
H	-5.15878769	0.86084240	-0.00014218
C	-5.10180765	-3.02372862	0.00001394
H	-2.95945524	-2.85773596	0.00010343
C	-6.31532919	-2.33252037	-0.00006195
H	-7.27072437	-0.39896319	-0.00017558
H	-5.09157780	-4.10653801	0.00005043
H	-7.24987611	-2.88004783	-0.00008237
C	3.90186256	-0.90745248	0.00001436
C	3.90114944	-2.31836865	0.00009635
C	5.13301234	-0.22149757	-0.00012744
C	5.10181311	-3.02372790	0.00003945
H	2.95946024	-2.85774154	0.00020208
C	6.32793996	-0.93201703	-0.00017720
H	5.15878231	0.86084342	-0.00020713
C	6.31533194	-2.33251716	-0.00009295
H	5.09158383	-4.10653719	0.00009842
H	7.27072315	-0.39895803	-0.00028641
H	7.24988114	-2.88004064	-0.00013312

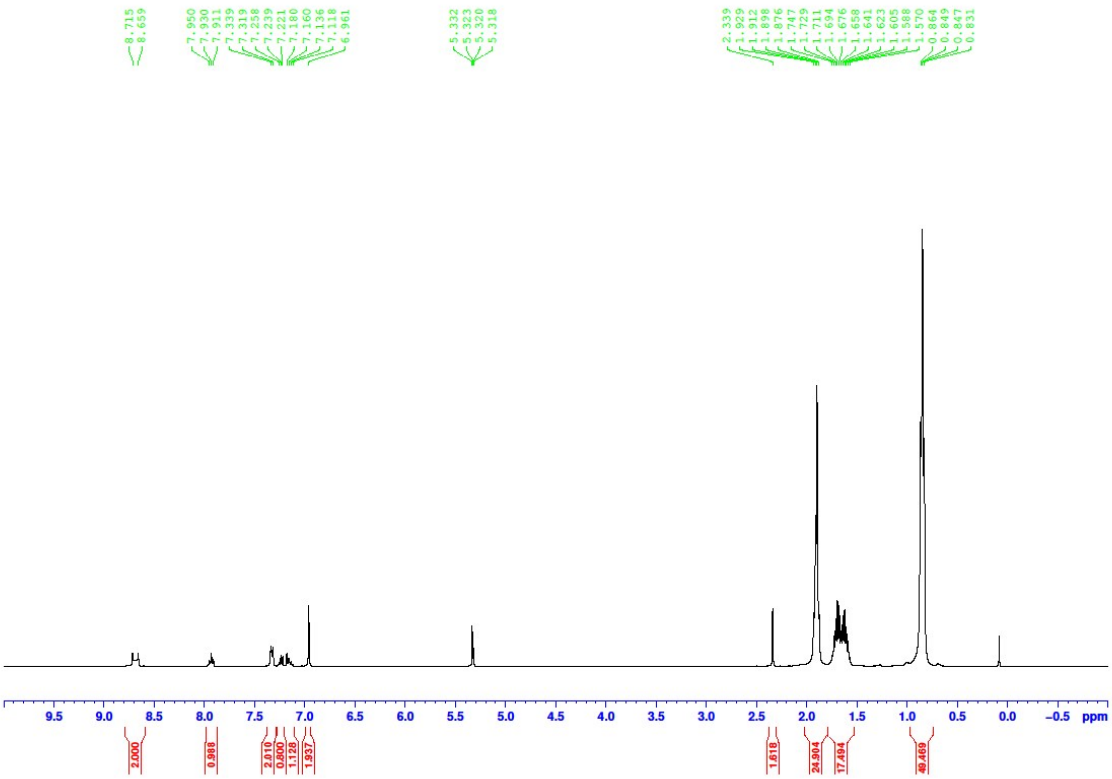

Fig. S1. ^{1}H NMR spectrum of **2** (400.13 MHz, CD_2Cl_2, 25 °C).

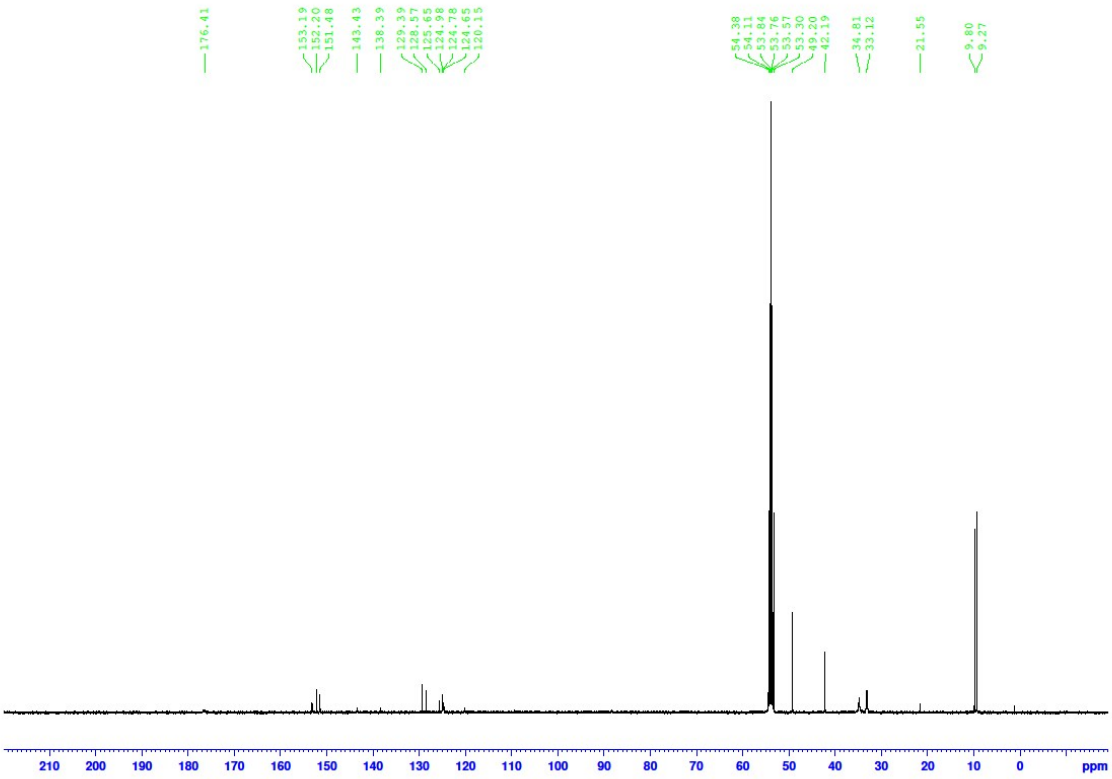

Fig. S2. ^{13}C NMR spectrum of **2** (100.62 MHz, CD_2Cl_2, 25 °C).

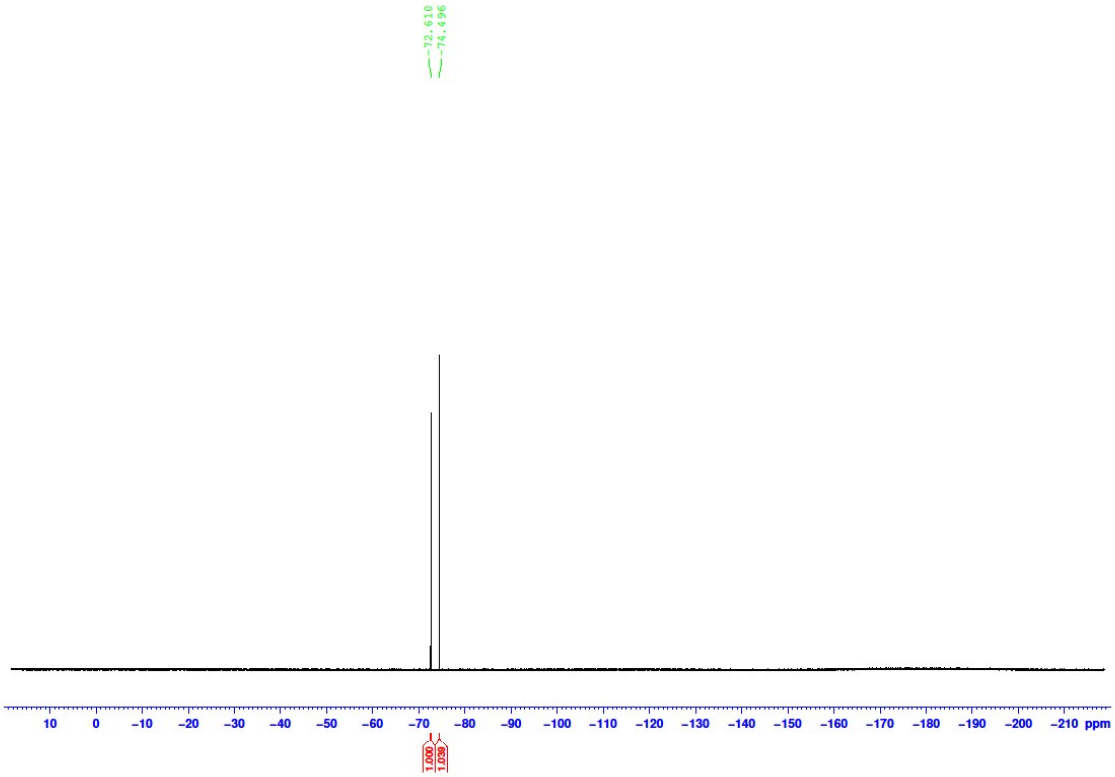

Fig. S3. ^{19}F NMR spectrum of **2** (376.46 MHz, CD_2Cl_2, 25 °C).

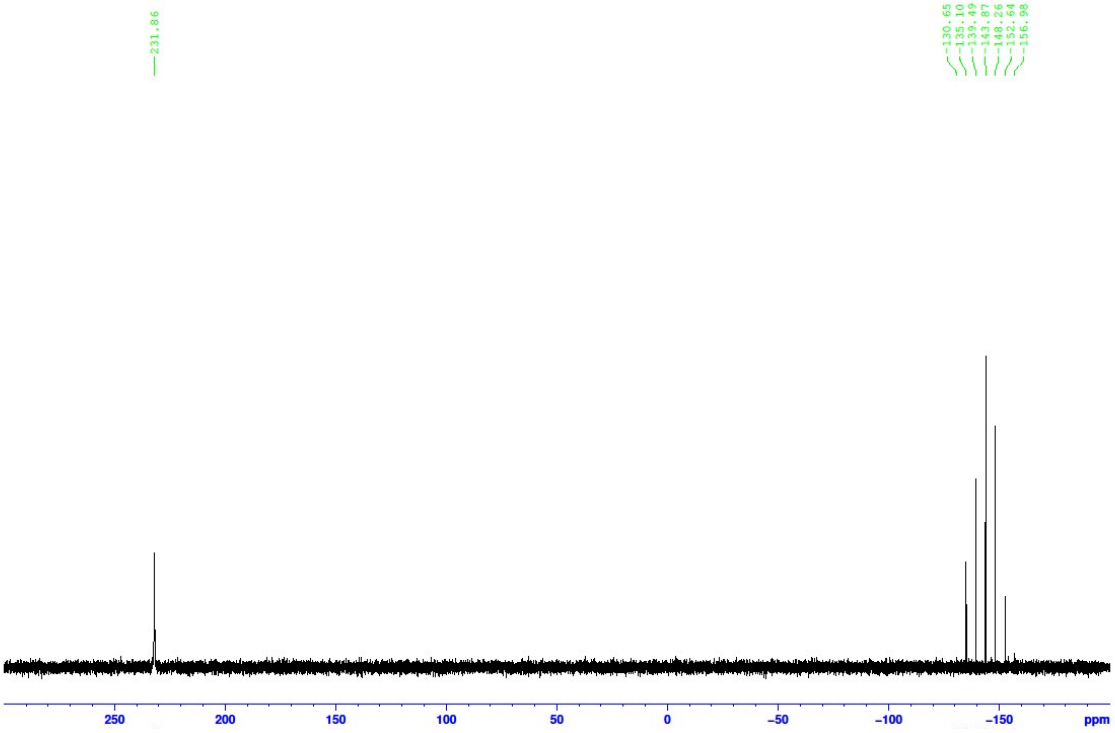

Fig. S4. ^{31}P NMR spectrum of **2** (161.98 MHz, CD_2Cl_2, 25 °C).

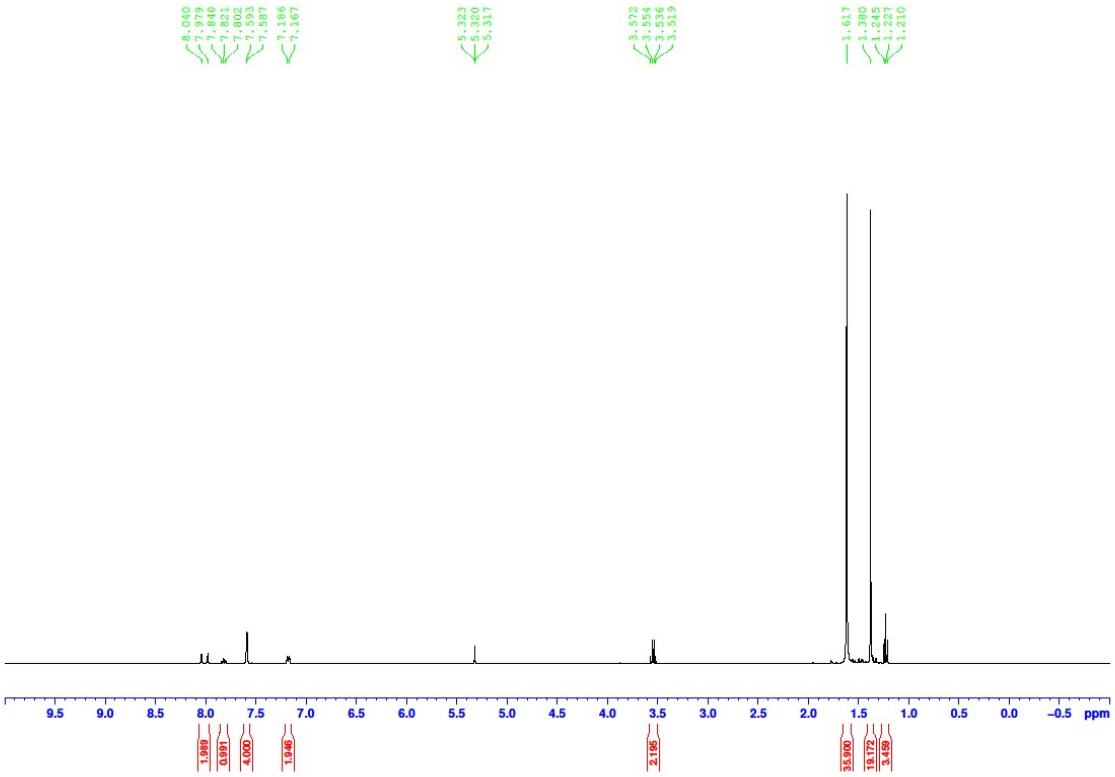

Fig. S5. ^{1}H NMR spectrum of **3**·OEt_2 (400.13 MHz, CD_2Cl_2, 25 °C).

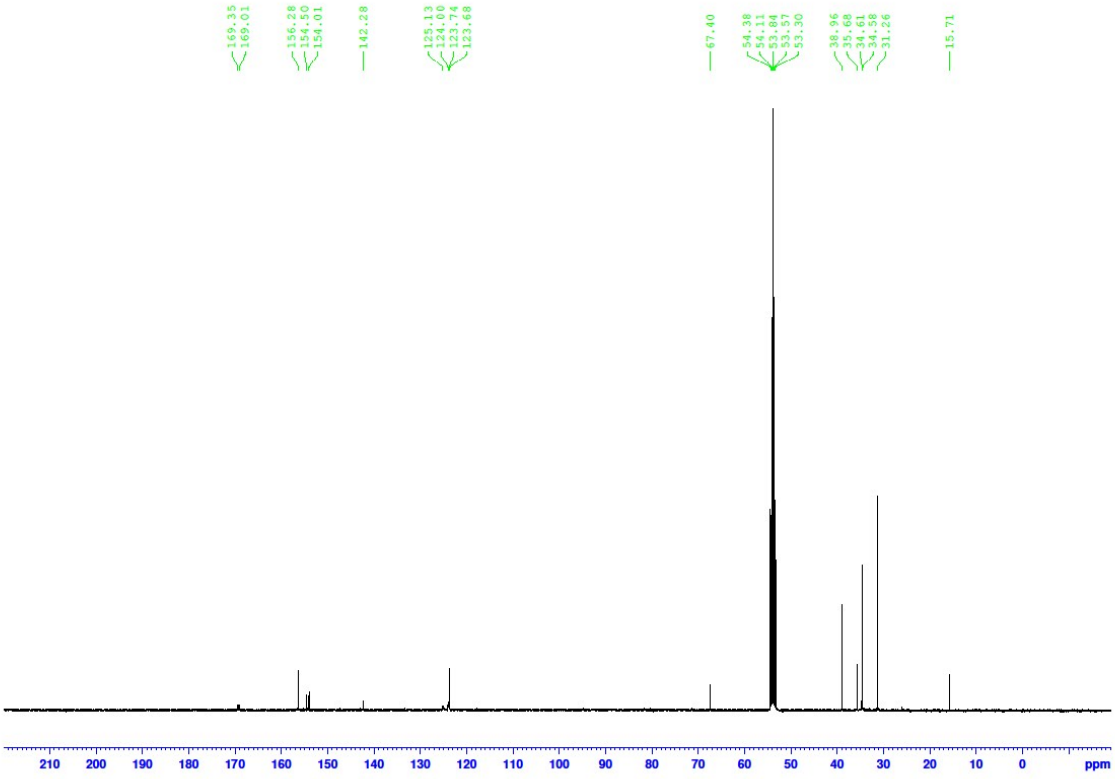

Fig. S6. ^{13}C NMR spectrum of **3**·OEt_2 (100.62 MHz, CD_2Cl_2, 25 °C).

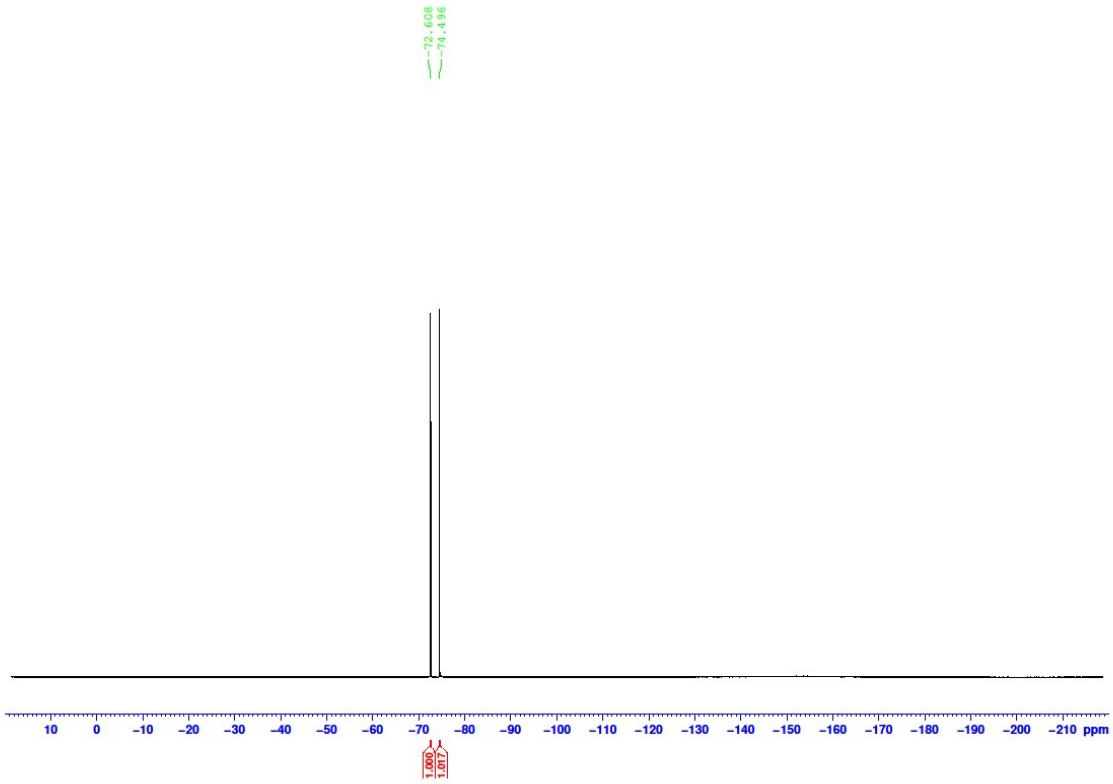

Fig. S7. ^{19}F NMR spectrum of **3**·OEt_2 (376.46 MHz, CD_2Cl_2, 25 °C).

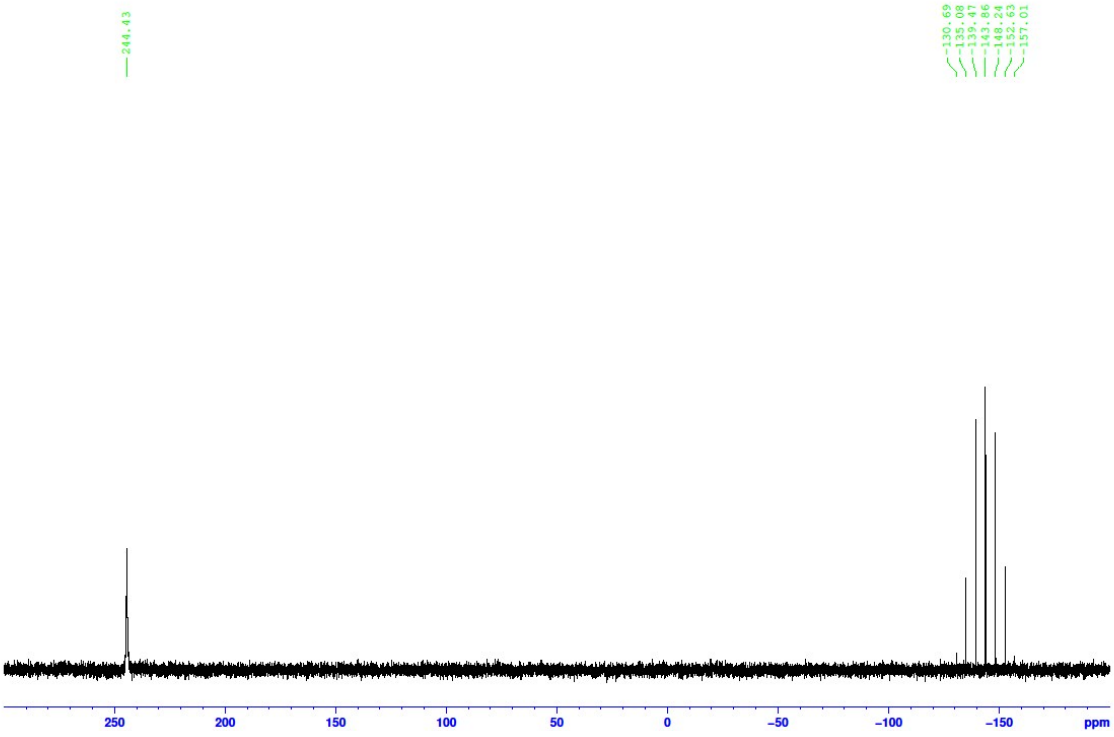

Fig. S8. ^{31}P NMR spectrum of **3**·OEt_2 (161.98 MHz, CD_2Cl_2, 25 °C).

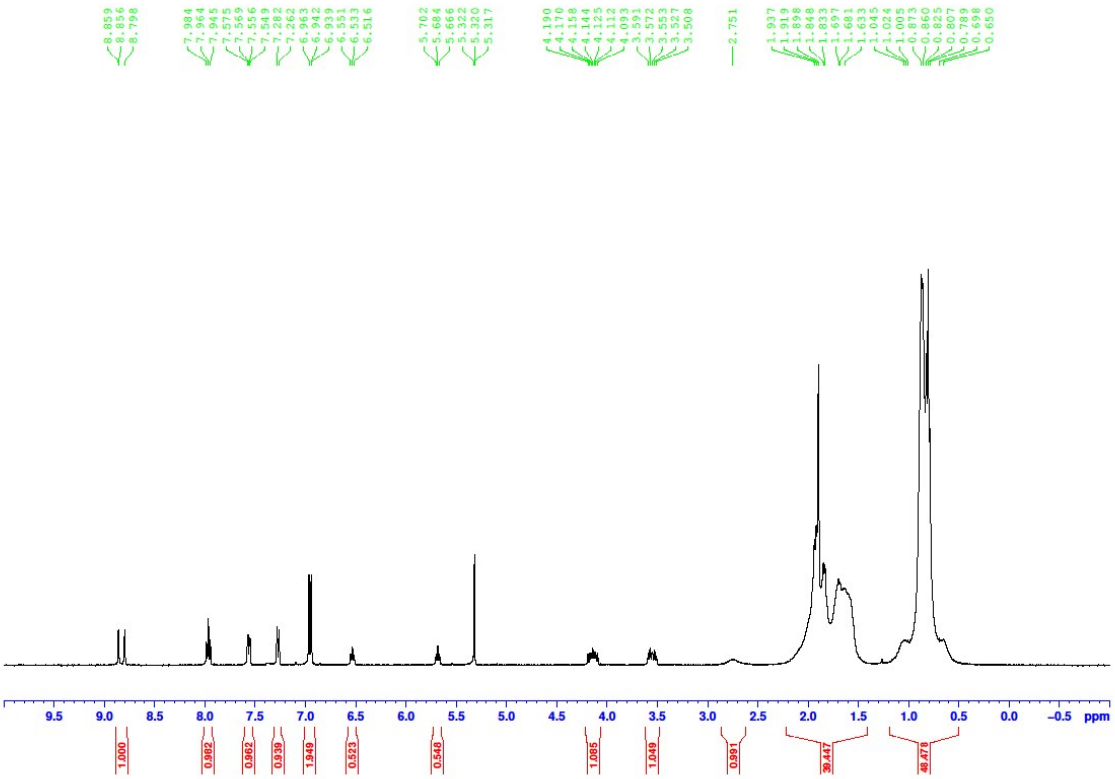

Fig. S9. ^{1}H NMR spectrum of **5** (400.13 MHz, CD_2Cl_2, 25 °C).

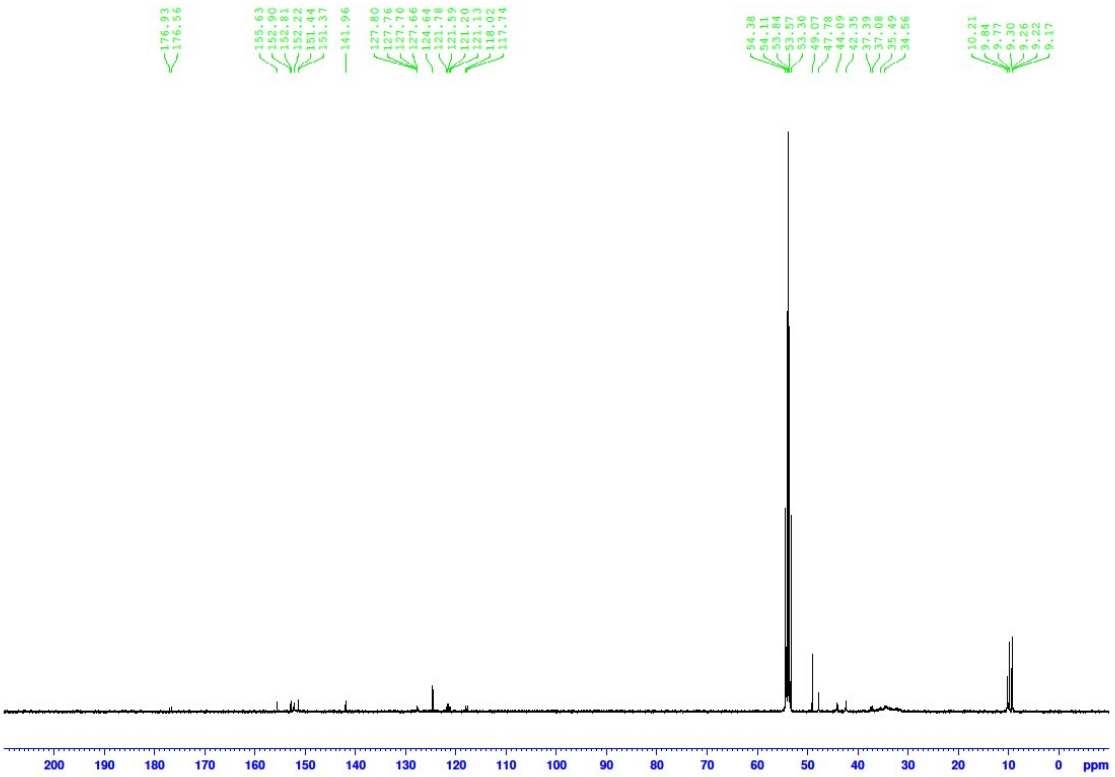

Fig. S10. ^{13}C NMR spectrum of **5** (100.62 MHz, CD_2Cl_2, 25 °C).

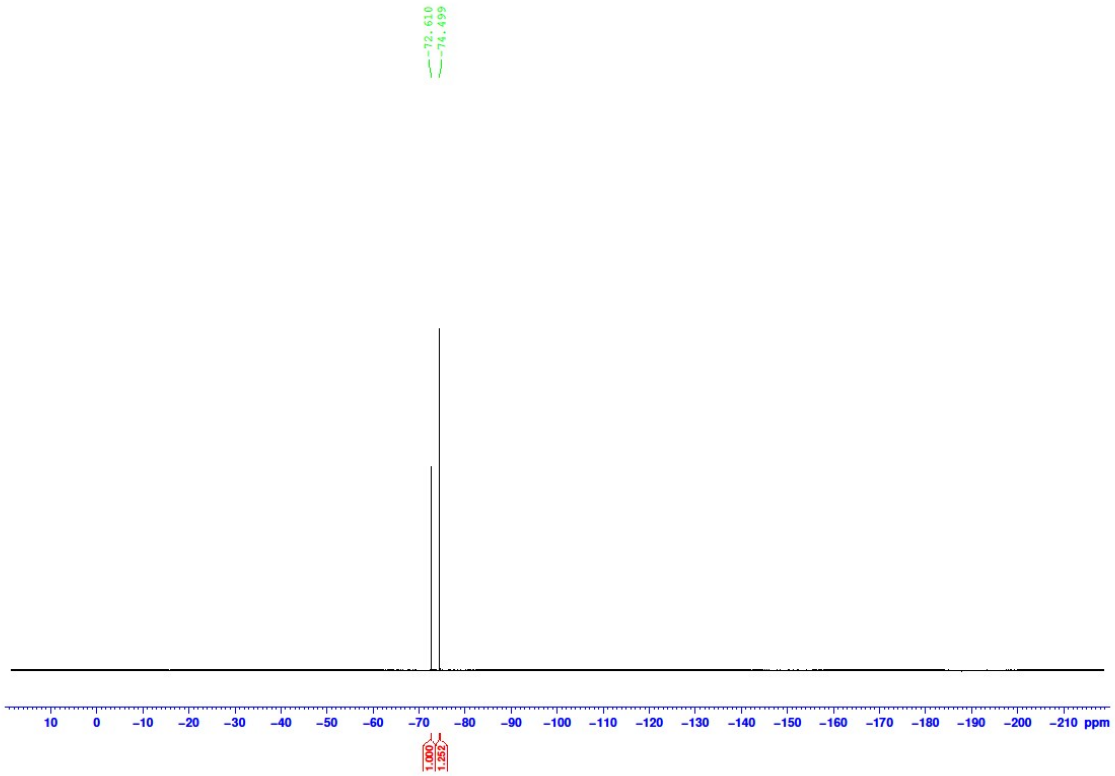

Fig. S11. ^{19}F NMR spectrum of **5** (376.46 MHz, CD_2Cl_2, 25 °C).

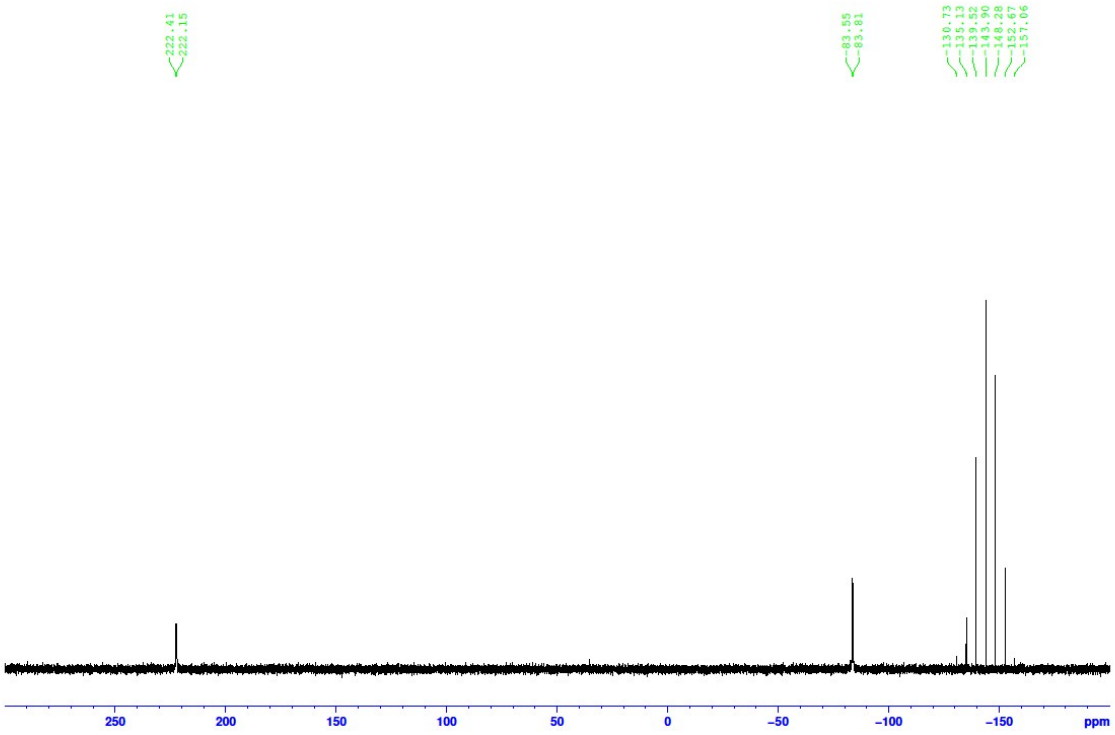

Fig. S12. ^{31}P NMR spectrum of **5** (161.98 MHz, CD_2Cl_2, 25 °C).

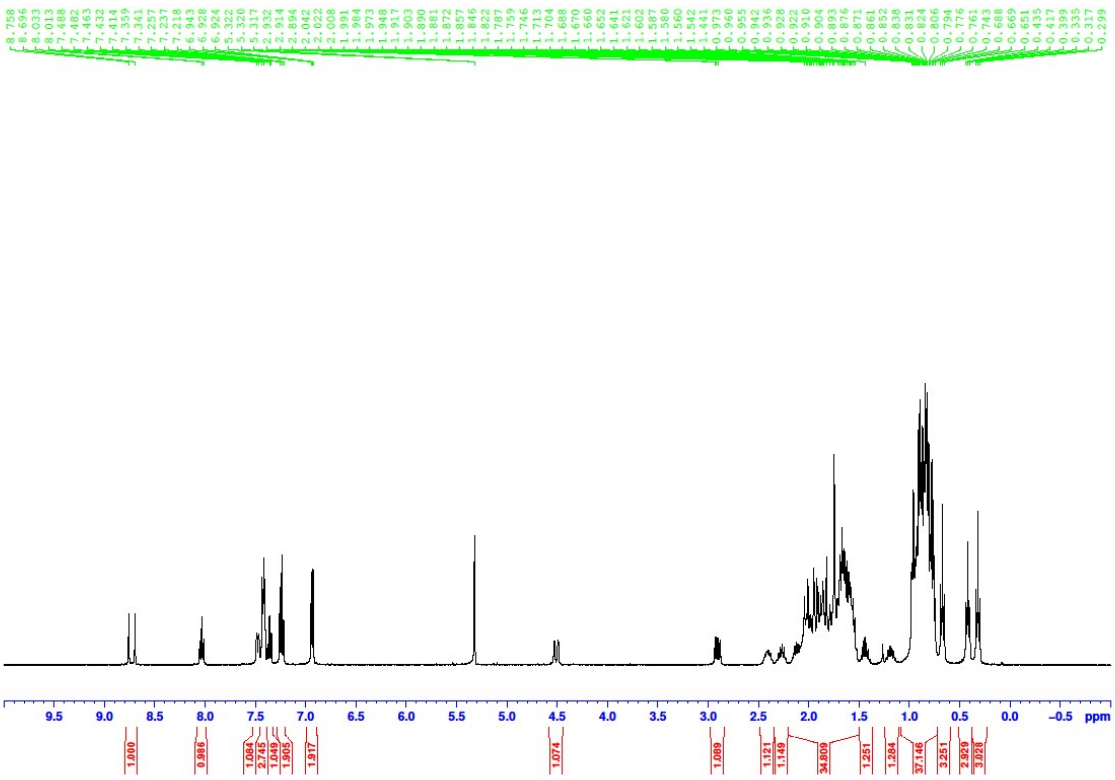

Fig. S13. ^{1}H NMR spectrum of **6** (400.13 MHz, CD_2Cl_2, 25 °C).

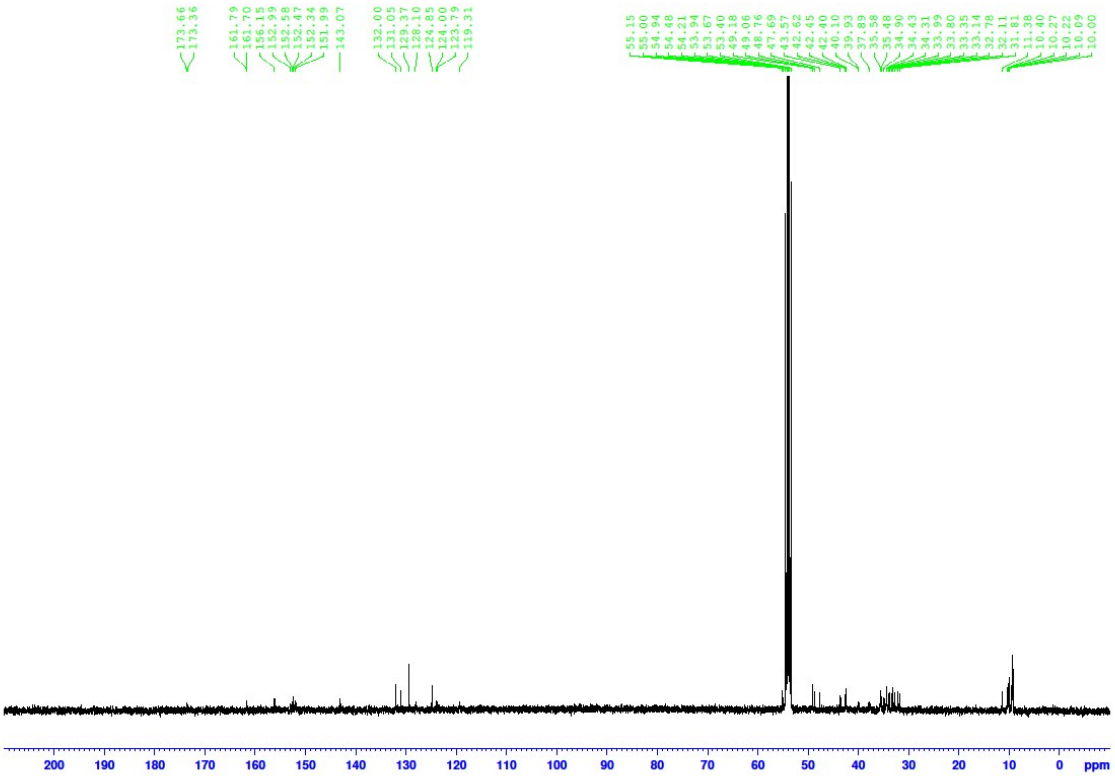

Fig. S14. ^{13}C NMR spectrum of **6** (100.62 MHz, CD_2Cl_2, 25 °C).

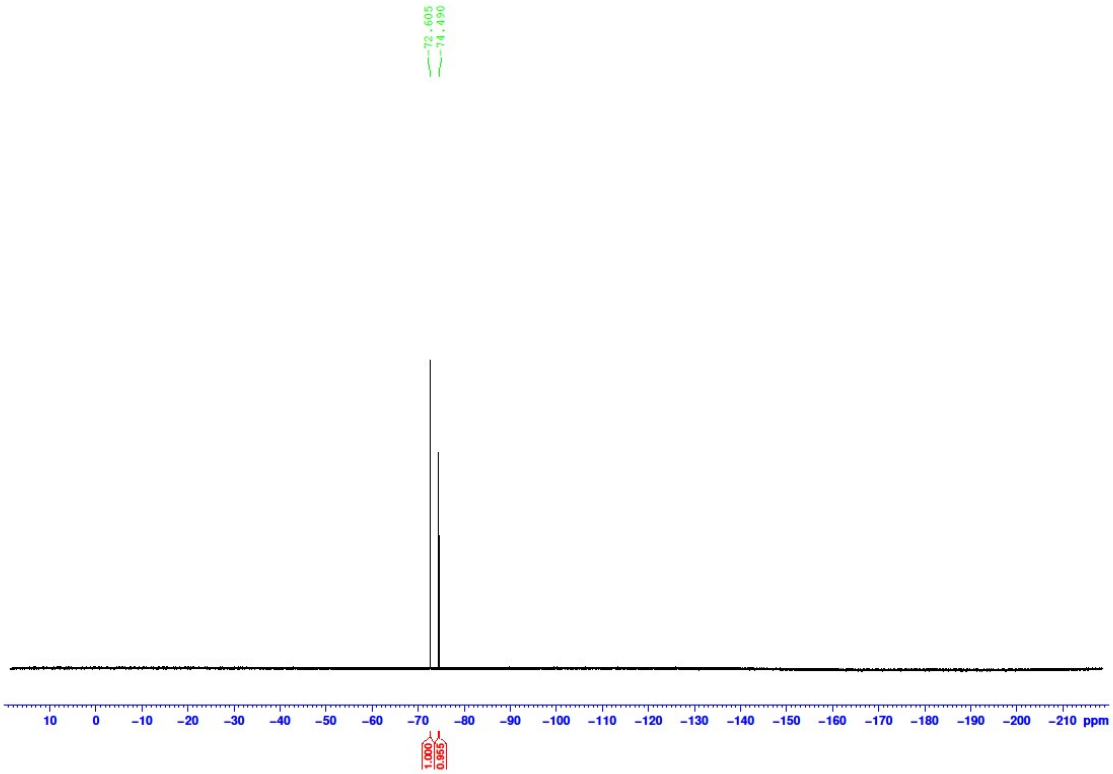

Fig. S15. ^{19}F NMR spectrum of **6** (376.46 MHz, CD_2Cl_2, 25 °C).

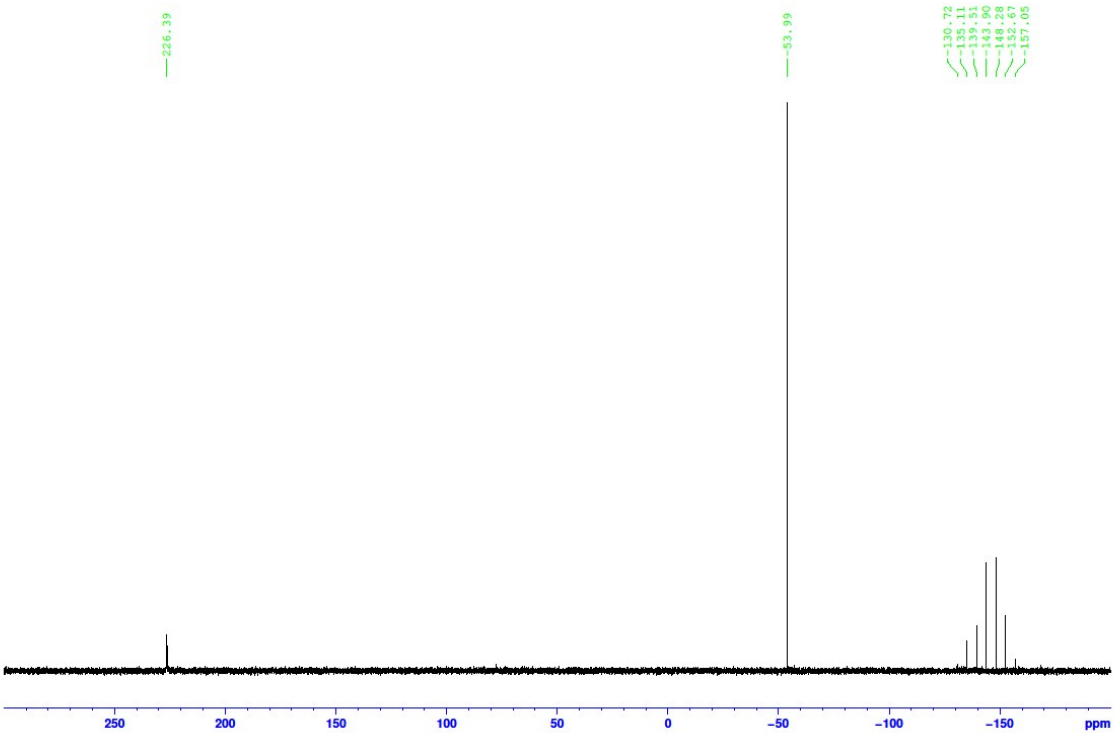

Fig. S16. ^{31}P NMR spectrum of **6** (161.98 MHz, CD_2Cl_2, 25 °C).